Journal of Molecular Medicine (2019) 97:1439–1450
https://doi.org/10.1007/s00109-019-01822-9

JMolMed

ORIGINAL ARTICLE

Bone allografts combined with adipose-derived stem cells in an optimized cell/volume ratio showed enhanced osteogenesis and angiogenesis in a murine femur defect model

Johannes M. Wagner[1] · Nicolas Conze[1] · Guido Lewik[1] · Christoph Wallner[1] · Jan C. Brune[2] · Stephanie Dittfeld[1] · Henriette Jaurich[1] · Mustafa Becerikli[1] · Mehran Dadras[1] · Kamran Harati[1] · Sebastian Fischer[3] · Marcus Lehnhardt[1] · Björn Behr[1]

Received: 27 September 2018 / Revised: 2 July 2019 / Accepted: 23 July 2019 / Published online: 31 July 2019

Abstract

Critical sized defects, especially in long bones, pose one of the biggest problems in orthopedic surgery. By definition, these defects do not heal without further treatment. Different therapeutic options range from autologous bone grafts, for example, free vascularized bone grafts, to commercially available bone allografts. Disadvantages of these bone allografts are related to reduced osteogenesis, since they are solely composed of cell-free bone matrix. The purpose of this study was to investigate the cell seeding efficiency of human adipose-derived stem cells (hASCs) on human bone allografts in vitro and furthermore analyze these optimized seeded allografts in a critical sized defect model in vivo. Cancellous human bone allografts were colonized with human ASCs in vitro. Cell seeding efficiency was evaluated by Cell Counting Kit-8 assay. Thereafter, optimized hASC-seeded bone scaffolds were examined in a murine femur defect model, stabilized with the MouseExFix system. Subsequently, x-ray analysis and histology were performed. Examination of cell seeding efficiency revealed an optimum starting population of 84,600 cells per 100 mm^3 scaffold. In addition, scaffolds seeded with hASCs showed increased osteogenesis compared with controls. Histological analysis revealed increased remodeling and elevated new bone formation within hASC-seeded scaffolds. Moreover, immunohistochemical stainings revealed increased proliferation, osteogenesis, and angiogenesis. In this study, we systemically optimized cell/volume ratio of two promising components of tissue engineering: hASCs and human bone allografts. These findings may serve as a basis for future translational studies.

Key messages

- Bone tissue engineering.
- Mesenchymal stem cells derived from human adipose tissue (hASCs).
- Optimal cell/volume ratio of cell-seeded scaffolds.
- Increased osteogenesis and angiogenesis in vivo.

Keywords Bone allograft · Scaffold; tissue engineering · Adipose derived stem cells

Johannes M. Wagner, Nicolas Conze and Guido Lewik contributed equally to this work.

Electronic supplementary material The online version of this article (https://doi.org/10.1007/s00109-019-01822-9) contains supplementary material, which is available to authorized users.

✉ Björn Behr
bjorn.behr@rub.de

[1] University Hospital BG Bergmannsheil Bochum, Bürkle-de-la-Camp Platz 1, 44789 Bochum, Germany

[2] Deutsches Institut für Zell- und Gewebeersatz, Berlin, Germany

[3] BG Trauma Hospital Ludwigshafen, Ludwigshafen, Germany

Introduction

Since the development of new tissue engineering techniques, progress has been made concerning critical sized defects in long bones. The use of scaffolds for bone replacement therapy has evolved over the past decade, utilizing a great variety of different scaffold materials [1–21], for example, collagen, chitosan, silk, alginate, hyaluronic acid, peptide hydrogels, and synthetic polymers like calcium phosphate and bioglass. All of these different scaffolds show adequate osteoconductive and biocompatible properties, but are limited in their usage due to lack of mechanical strength [22]. Moreover, scaffolds composed of synthetic materials are not osteoinductive or osteogenic by themselves [23]. Some of these disadvantages can be overcome by human bone allografts. Besides the fact that these cell-free and therefore biocompatible bone allografts are commercially available in adequate numbers, they provide both good osteoconductive properties and mechanical strength and show adequate osteointegration [22, 24]. Contrarily, potential immunogenic reactions of implanted allografts caused by activation of the major histocompatibility complex (MHC) have been described, which can lead to apoptosis of infiltrating osteoprogenitor cells. [25]. Moreover, the use of bone allografts poses the risk of viral transmission, which could already be improved by modern tissue banks [26].

It is well-accepted that all scaffolds, despite their different basic materials, fall short when it comes to new bone formation within the scaffold. This is mainly attributable to the lack of living cells. Therefore, combining suitable scaffolds with multipotent stem-cell populations is one promising option to solve this problem [22, 24, 27, 28]. In this context, particular attention has already been paid to adipose-derived stem cells (ASCs). They are easily accessible and available to an almost unlimited amount. Studies suggest that bone allografts combined with ASCs could improve osteogenesis and angiogenesis [28, 29]. Although the combination of ASCs and bone allografts seems promising for bone replacement therapy, only little is known about the seeding efficiency of mesenchymal stem cells and scaffolds with an optimized cell/volume ratio. Therefore, this study aimed to examine different numbers of ASCs seeded on bone allografts in order to identify the most efficient cell/allograft ratio. Moreover, optimized hASCs-seeded scaffolds were tested in vivo in a murine femur defect model.

Methods

In order to examine scaffolds co-cultured with ASC's for bone replacement therapy, our first aim was to analyze and optimize cell seeding efficiency. Therefore, we analyzed human allogenic spongiosa chips seeded with undifferentiated human ASCs in vitro.

Utilizing the ideal ratio of cells and volume, we subsequently studied the bone regeneration capacity of these seeded scaffolds in a murine animal model in vivo.

Isolation and characterization of human ASCs

All experiments were performed in adherence to the institutional ethical review board with the permit number 4689-13.

For isolation of adipose-derived stem cells, fat tissue from seven male and female patients was used (age 32–49 years). The fat tissue was obtained from abdominoplastic surgery. The selected patients had no relevant diseases and were all non-smokers.

After separation of subepidermal fat tissue from dermis and disintegration, specimens were incubated with collagenase IV solution.

After filtration and centrifugation of the suspension, cells were resuspended in lysis buffer for lysis of erythrocytes. After stopping lysis with DMEM-medium (DMEM + 45% Ham's F12 + 1% penicillin, streptomycin + 10% FCS), cell suspension was again centrifugalized. Cell pellets were resuspended in medium subsequently and cells were seeded on cell culture plates (5% CO_2, 37 °C). For further characterization of the isolated cell population, we performed FACS analysis. To prevent non-specific binding, Fc receptors were blocked with anti-CD16/CD32 antibodies (BD Pharmingen, San Diego, USA) before cells were stained with antibodies against CD90, CD14, CD45, CD34, CD105, and CD11b. Flow cytometry was carried out using BD LSRFortessa and corresponding software to compensate fluorescence intensity of antibodies. Results of FACS analysis indicated 95% mesenchymal stem cells within used cell population.

Results are presented as the mean of at least 7 independent experiments utilizing hASCs of all seven donors.

Seeding of scaffolds

For all experiments, human cancellous bone scaffolds (GT2803, DIZG, Berlin, Germany) were utilized. Isolated human adipose-derived stem cells were counted with CASY-Ton system (Omni-life science, Bremen, Germany) right before seeding of the scaffolds. First, scaffolds were placed in 24-well plates and seeded with 60 μl FCS containing 0 to 500,000 cells subsequently. Finally, 1 ml of medium was added and scaffolds were returned to the incubator.

For cell proliferation in vitro experiments (P1) and in vivo experiments, cells were incubated in standard medium.

For osteogenic differentiation in vitro experiments (P2), cells were incubated in osteogenic differentiation medium (DMEM + 10%FCS + 45% Ham's F12 + 1% penicillin, streptomycin + 10 mM betaglycerolphosphate + 5 nM

dexamethasone + 150 μM ascorbic acid) in order to perform histological analysis of the seeded scaffolds.

Analysis of vital cell number

In order to examine the seeding efficiency of scaffolds, different starting cell populations were evaluated within the first phase of in vitro experiments (P1). Scaffolds with a capacity of 295.5 mm^3 were placed into 24-well plates and seeded with 0, 10,000, 50,000, 100,000, 200,000, 250,000, 300,000, and 500,000 cells as described above. Number of vital cells was evaluated on day 0, 1, 7, 14, and 21 after initial cell seeding, using cell counting kit 8 (Sigma Aldrich, St. Louis, USA) according to the manufacturer's instructions. On designated time points, scaffolds were incubated in 700 μl PBS containing 70 μl of CCK-8 reagent for 3 h at 37 °C and 5% CO_2. Then 100 μl was pipetted into 96-well plate and extinction was measured at 450 nm.

Animal model

All experiments were performed in adherence to the National Institute of Health guidelines for the use of experimental animals and after approval by the German legislation.

The protocol was approved by the LANUV (NRW, Germany; Permit-Number: AZ 84-02.04.2013.A362). For in vivo experiments, 12-week-old male and female athymic CD1 mice (Charles River (Wilmington (MA), USA)) were used. Surgical steps were performed, as previously described [30].

Briefly, a skin incision was performed along the lateral upper leg, exposing the greater trochanter. Then a second incision was performed along the fascia lata and the quadriceps femoris muscle was mobilized to expose the femur. Thereafter, the first pin hole (0.45-mm diameter) was drilled into the distal femur. The first pin, inserted into plastic body of external fixation device, was then placed into the hole penetrating the lateral and medial cortex of the femur. Finally, three holes were drilled and pins were inserted into the remaining holes of the plastic device, placing the external fixation device. Thereafter, two Gigli wires were placed around the femur within the preformed saw guide of the plastic body and a defect of 3 mm was cut into the femur. Thereafter, scaffolds prepared with ASCs (experimental group) and PBS (control group) were placed into the defect. Then, the quadriceps femoris muscle was reapproximated and skin was sutured.

Mice were sacrificed after 48 h and 8 weeks and femurs were taken for histological and x-ray analysis. A total of 25 animals were used for experiments with a minimum of four animals per group.

Figure 1 summarizes the surgical procedures performed.

Histology, immunohistochemistry, and immunofluorescence

For histological analysis, bone specimens and scaffolds were harvested and fixed in 4% paraformaldehyde solution, decalcified in 19% EDTA solution, and finally paraffin embedded. Thereafter, specimens were longitudinally sectioned with a microtome at 9 μm. Thereafter, Aniline blue staining was performed after standard protocols and stained pixels were counted semiautomatically, using Adobe Photoshop, as previously described [31–33]. In order to distinguish between newly formed bone and the scaffold itself, we performed combined Aniline blue and immunohistochemical stainings against osteocalcin as described below.

Moreover, HE stainings were performed after standard protocols. For detection of apoptotic cells, in situ cell death detection kit (Roche Diagnostics, Mannheim, Germany) was used according to the manufacturers' instruction.

Additionally, immunohistochemical stainings were performed, using primary antibody against osteocalcin anti-mouse (Santa Cruz Biotechnologies, Dallas, USA), CD31 anti-mouse (BD Pharmingen, San Diego, USA), CD31 anti-human (DAKO, Santa Clara, USA), mitochondria anti-human (Abcam, Cambridge, UK), PCNA anti-mouse (Santa Cruz Biotechnologies, Dallas, USA), and Vectastain ABC Kit (Vector Laboratories, Burlingame, USA). For antigen unmasking, Proteinase K was used. Then incubation with 3% hydrogen peroxide solution was followed quenching endogenous peroxidase activity. After blocking specimens with normal blocking serum, primary antibody was subsequently applicated and incubated overnight at 4 °C. Thereafter, secondary antibody conjugated to horseradish peroxidase (HRP) was used and staining reaction was performed by use of NovaRED (HRP) Peroxidase Substrate Kit (Vector Laboratories, Burlingame, USA).

Immunofluorescent stainings were performed using primary antibodies against RUNX2 anti-mouse (Santa Cruz Biotechnologies, Dallas, USA). First steps were performed similar to immunohistochemical staining until application of primary antibody. Then, samples were incubated with secondary antibody conjugated to Alexa Fluor594 (Thermo Fisher Scientific, Waltham, USA). Finally, images were taken with Zeiss Axioplan microscope.

Statistics

Results are presented as mean ± standard deviation (SD) of at least three independent experiments. Student's t test was used calculating p value, comparing two groups. For

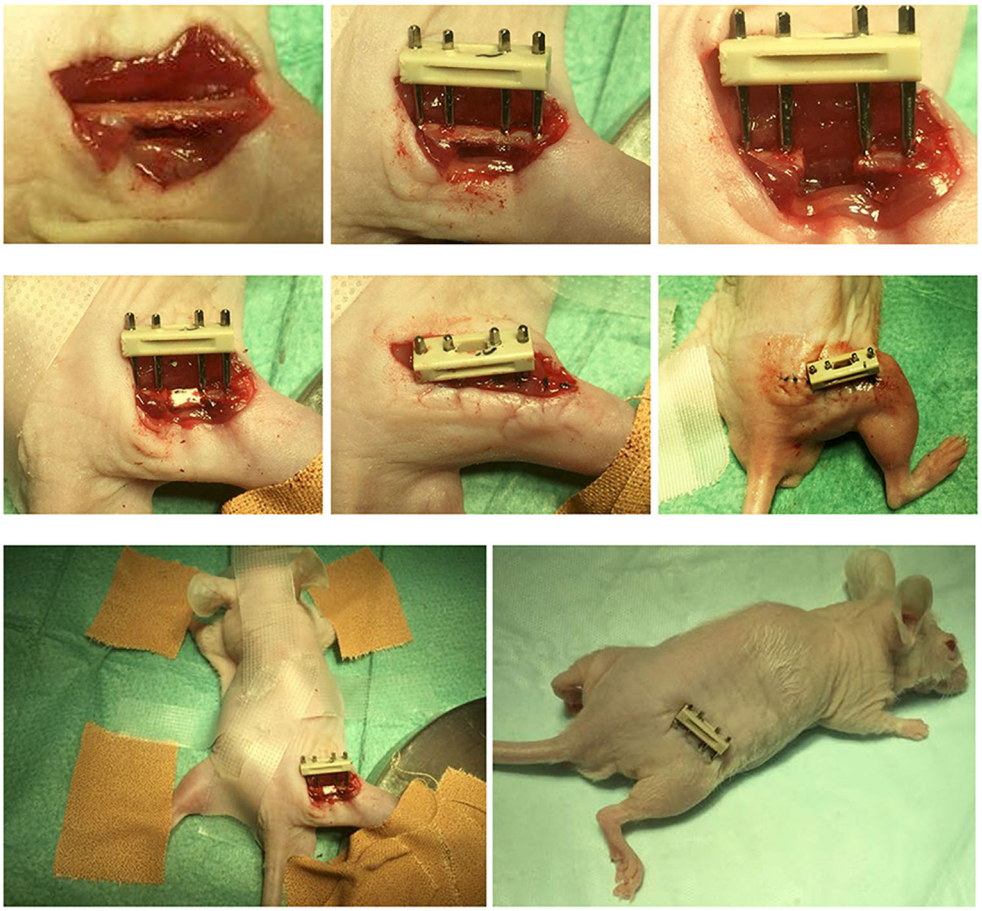

Fig. 1 Surgical procedures of femoral defect model. The right femur was stabilized via Mouse ExFix System (RIS-Systems) and 3 mm defect was created. Thereafter, hASC seeded scaffold was placed into defect

comparison of more than two groups, ANOVA was used. For post hoc analysis, Tukey's test was used. Statistical significances were set at a p value < 0.05.

Results

Vital cell population of scaffolds increases with starting cell number

In order to examine cell-seeded scaffolds with ideal conditions in vivo, we first had to determine the optimal starting cell number. In groups with initial seeding cell numbers between 10,000 and 250,000 cells, a statistically significant increase of vital cells could be observed from day 0 to day 21 (see Fig. 2). Interestingly, final cell numbers at day 21 of groups with starting seeding cell numbers between 250,000 cells and 500,000 showed no statistically significant differences (Fig. 2b). Moreover, comparing cell numbers at day 21, statistically significant differences in vitality could be found between a starting population of 50,000 and 250,000 cells (Fig. 2a–d). Furthermore, a distinct vitality increase of cell numbers at day 21 could be observed between 200,000 and 250,000 cells, however not statistically significant.

High starting populations create densely populated scaffolds

After examining different starting populations over a period of time, we were interested how seeded stem cells populate the scaffolds. Thus, HE stainings, as well as DAPI and TUNEL stainings, were performed to have a more detailed look on cell colonization.

As expected, higher starting cell numbers created scaffolds densely populated with cells. Comparing 10,000 cells and 250,000 cells in HE staining (see Fig. 3a–c), remarkable differences could be observed, i.e., almost absence of cells on the one hand and thick cell bonds on the other. These cell bonds were also localized between the trabeculae (Fig. 3c).

DAPI and TUNEL stainings confirmed these observations, displaying only scattered apoptotic cells in group of 100,000 and 250,000 cells (Fig. 4). Interestingly, these TUNEL positive signals could only be found localized directly on the scaffolds and not adjacent to them, indicating vivid cells adjacent to the scaffolds.

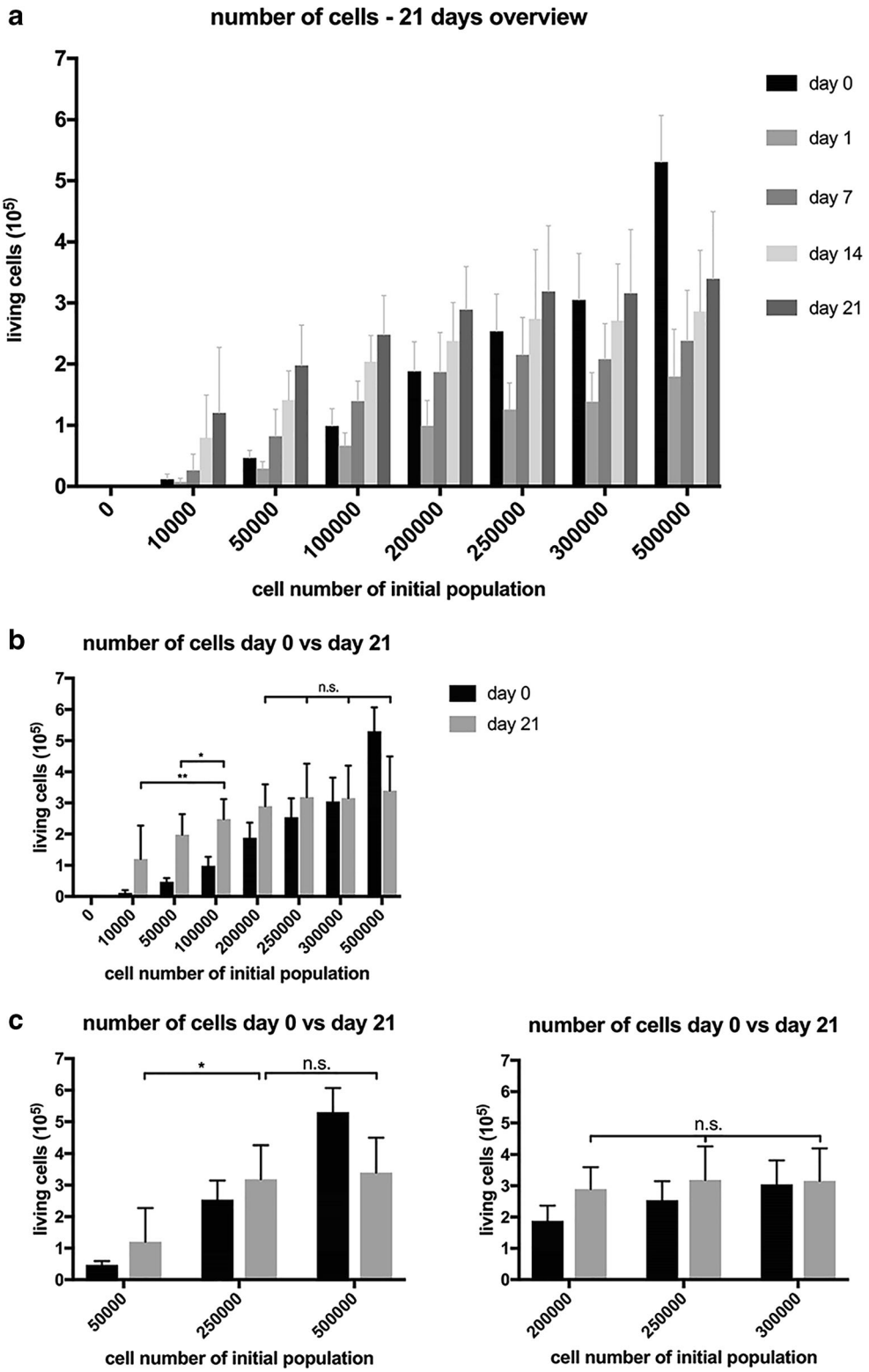

Fig. 2 **a**–**d** Cell vitalitiy evaluated by CCK-8 kit. Scaffolds were seeded with different starting cell populations between 0 and 500,000 cells of seven different donors. Cell vitality was measured at days 0, 1, 7, 14, and 21 and average of all donors is shown. Interestingly, number of cells measured at day 21 could only be raised up to 250,000 cells. Cell vitality of different groups at 21 days showed statistically significant differences between 50,000 and 250,000 cells. *P value < 0.05, **P value <0.01; n.s. stands for not significant

Combination of hASCs and scaffolds increase new bone formation in vivo

Findings from our in vitro examinations presented above lead to an optimal starting population of 250,000 cells per scaffold, resulting in a ratio of 84,600 cells/100 mm^3.

In order to investigate, how these optimized hASCs-seeded scaffold regenerate bone in vivo, they were implanted in critical sized defects of athymic

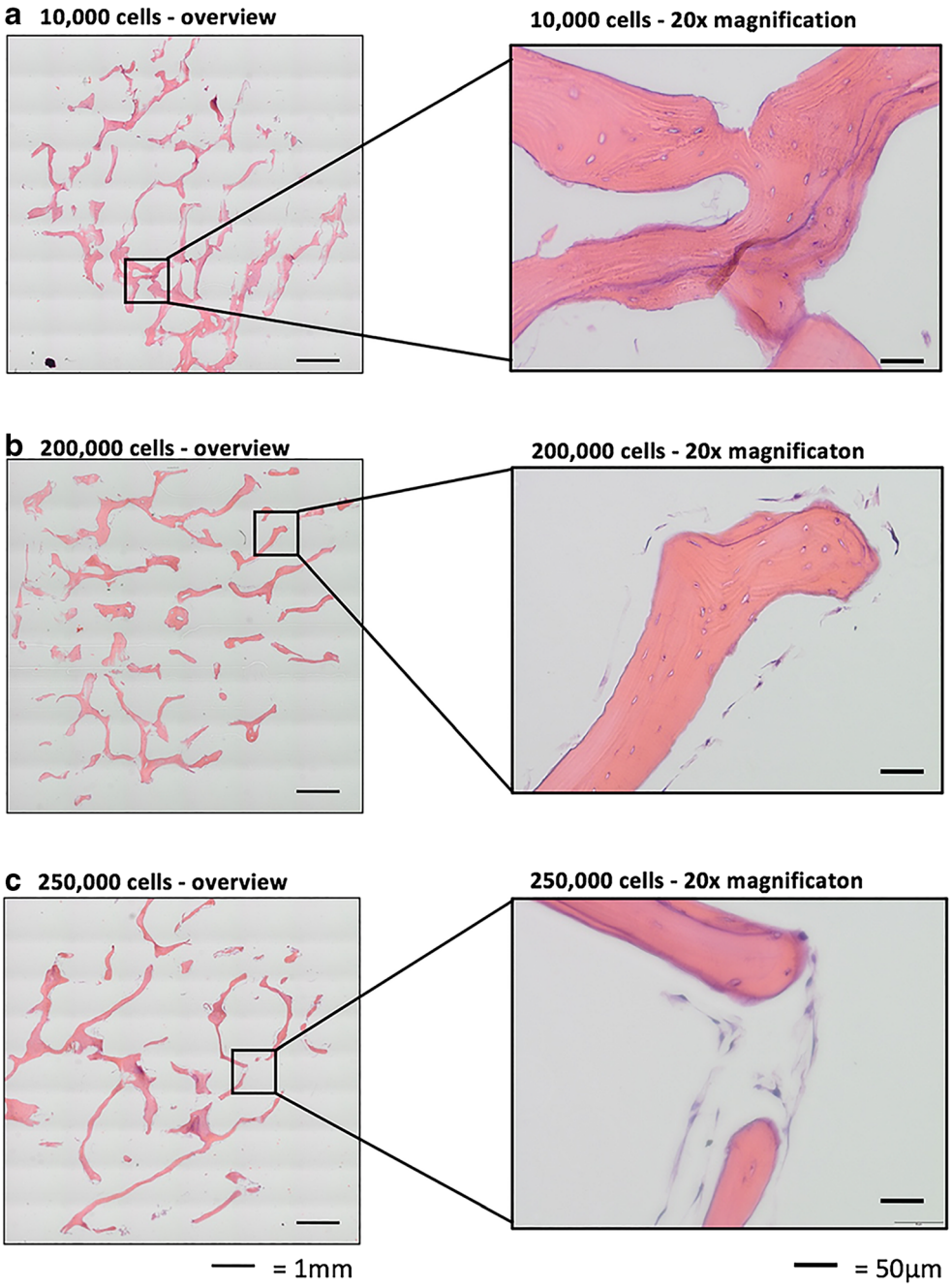

Fig. 3 HE staining of cell-seeded scaffolds. Lower starting cell populations showed hardly any cells located on the scaffold after observation period (**a**). Higher cell numbers could form thick cell layers on the scaffold (**b**, **c**). Images of HE stainings were taken at × 20 magnification

nude mice. New bone formation evaluated by Aniline blue staining showed a highly significant elevation in hASC group, compared with control (see Fig. 5). Comparing scaffold structures of hASC and control groups, combination of stem cells could significantly improve integration of scaffolds into bony defects.

Moreover, immunohistochemical stainings with primary antibody against Runx2 and osteocalcin showed enhanced osteoblastogenesis and elevated number of osteoblasts in experimental group compared with control (Fig. 6).

Applicated hASCs differentiate into endothelial cells

Immunohistochemical stainings were performed against mouse and human CD31 and human mitochondrias to track the transplanted human stem cells and investigate angiogenic differentiation. Interestingly, stainings with primary antibodies against CD31 showed endothelial differentiation for mouse as well as human cells. This indicates paracrine as well as cell-autogous effects of hASCs on angiogenesis in this model (Figs. 6 and 7). In PCNA stainings, significant differences of seeded and unseeded scaffolds could be seen at 48 h

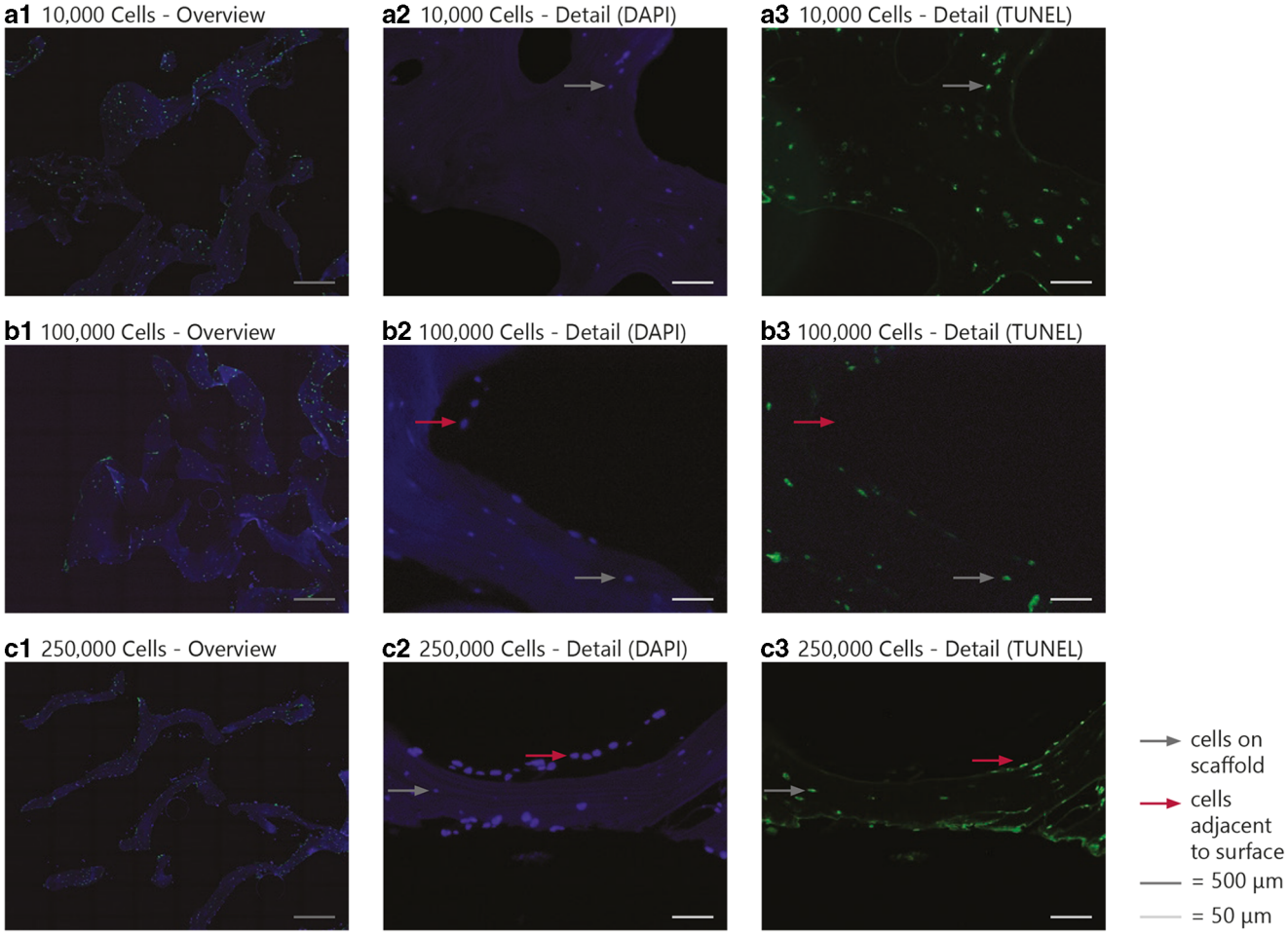

Fig. 4 DAPI and TUNEL stainings of low and high cell numbers. Stainings of lower cell numbers revealed scant vital cells on scaffold (A) in comparison with higher cell numbers (B, C). Interestingly, vital cells stained by DAPI seemed to surround the scaffolds (indicated by red arrows) while TUNEL positive signals were only located on the scaffold (indicated by gray arrows). Images were taken at × 20 magnification

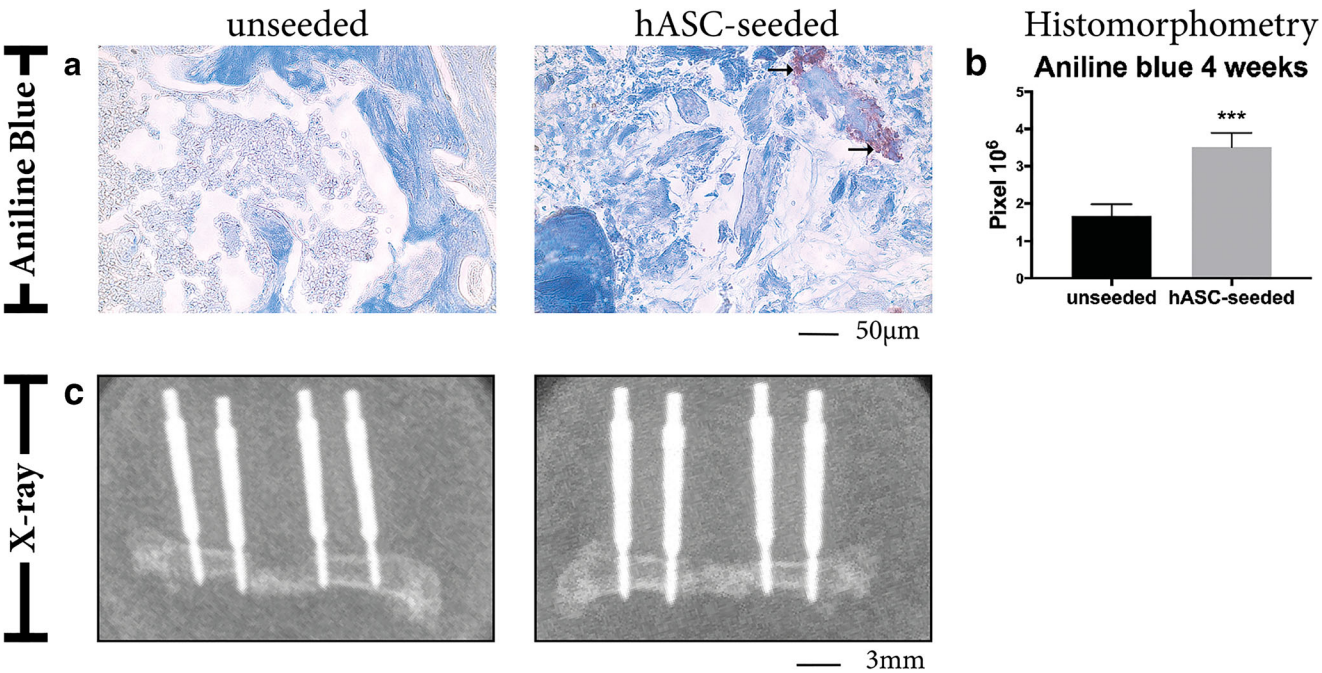

Fig. 5 Aniline blue, osteocalcin stainings, and x-ray scans of hASC-seeded and unseeded scaffolds.

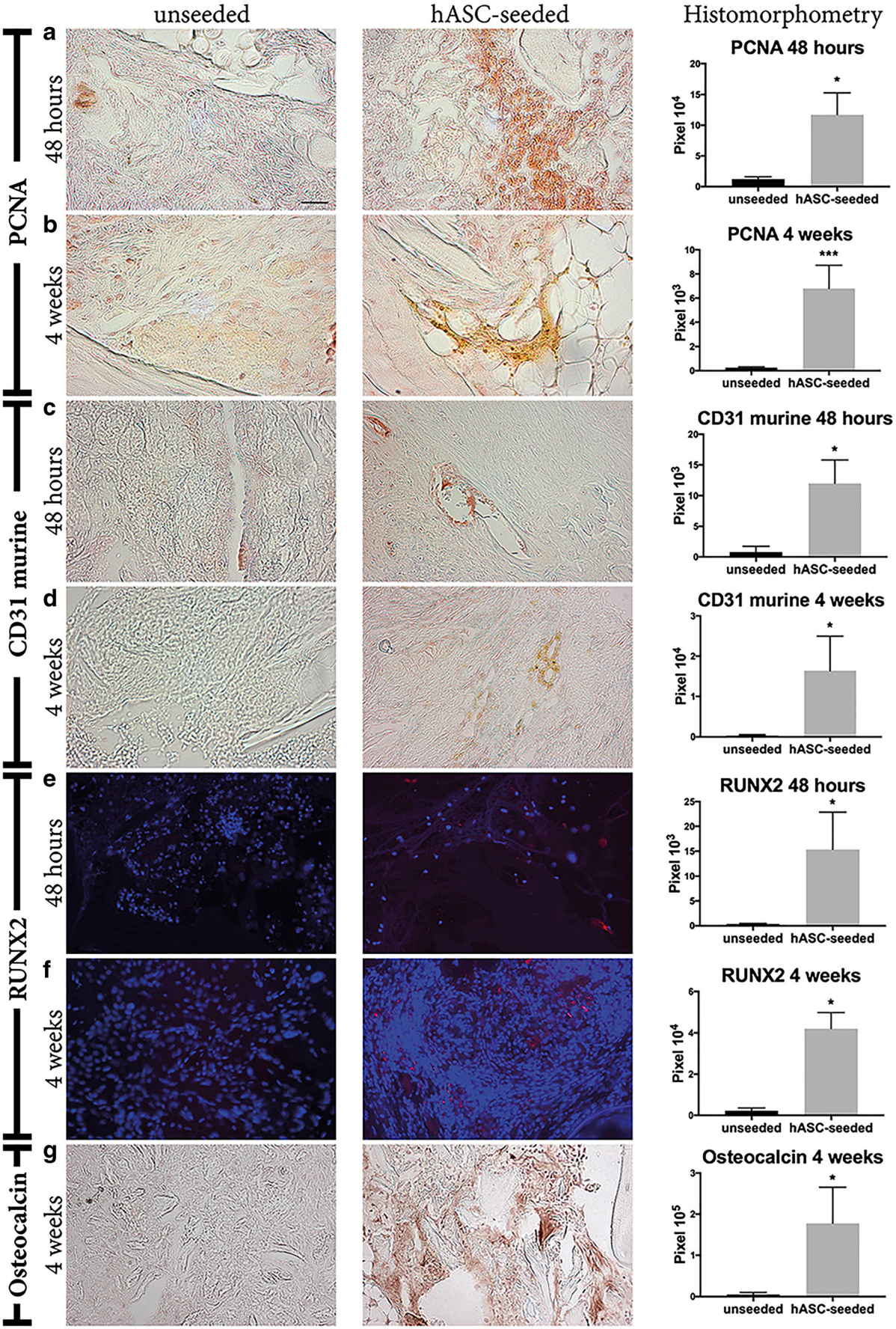
unseeded
hASC-seeded
Histomorphometry
PCNA
CD31 murine
RUNX2
Osteocalcin
a
48 hours
b
4 weeks
c
48 hours
d
4 weeks
e
48 hours
f
4 weeks
g
4 weeks
PCNA 48 hours
Pixel 10^4
unseeded hASC-seeded
PCNA 4 weeks
Pixel 10^3
unseeded hASC-seeded
CD31 murine 48 hours
Pixel 10^3
unseeded hASC-seeded
CD31 murine 4 weeks
Pixel 10^4
unseeded hASC-seeded
RUNX2 48 hours
Pixel 10^3
unseeded hASC-seeded
RUNX2 4 weeks
Pixel 10^4
unseeded hASC-seeded
Osteocalcin 4 weeks
Pixel 10^5
unseeded hASC-seeded

◀ **Fig. 6** **a**–**g** Immunohistochemical stainings against mouse antigen of seeded and unseeded scaffolds. Osteocalcin and RUNX2 stainings depicted enhanced osteogenesis of hASC-seeded scaffolds in comparison with unseeded control. Stainings with antibodies against CD31-mouse revealed increased angiogenesis within the scaffold. Enhanced proliferation of seeded scaffolds was proven by PCNA staining. Results are shown as mean ± SD. **P* value < 0.05. ****P* value < 0.001. Images were taken at × 20 magnification; scale bar represents 50 μm

and 4 weeks. Interestingly, PCNA signal of seeded scaffolds dropped over time course (see Fig. 6). Moreover, stainings against human mitochondrias (hmito) showed increasing signal over time in the hASC-seeded scaffold group, which might be related to increased numbers of hASCs within the scaffold after 4 weeks (Fig. 7). Of note, hmito stainings of unseeded scaffolds showed no signal (data not shown).

Discussion

Given the challenges encountered by critical sized defects in long bones, caused by trauma, tumors, or severe infections, there is an urgent and so far unmet need for sufficient reconstructive options. As bone allografts pose excellent osteoconductive qualities, combined with mechanical strength [22, 34], it seems reasonable to use their natural reconstructive capacity and enhance the osteoinductive outcome by combining them with mesenchymal stem cells. Therefore, this study focused on an optimized cell/volume ratio of ASCs and bone allografts and moreover evaluated the cell conductivity and the regenerative capacity of bone allografts, examined by new bone formation, angiogenesis, and cell proliferation.

Searching for an adequate scaffold for bone replacement therapy, Seebach et al. compared different biological and synthetic scaffold materials [34]. Interestingly, bone allografts showed best characteristics regarding cell conductivity as opposed to all other scaffolds, presumably because of the collagen-fiber structure. Based on these findings, we used spongiosa chips seeded with ASCs as this combination seemed to be superior to synthetic scaffold materials regarding bone replacement therapy. Furthermore, in comparison with other mesenchymal stem cells, ASCs are easily obtainable to an almost unlimited extend with only little donor site morbidity [35].

Thus, it was the aim of this study to identify the ideal number of ASCs combined with bone allografts and examine the bone healing capacity based on these findings, in vivo.

Within the first phase of experiments, we could show that a ratio of 84,600 cells per 100 mm^3 scaffold is advantageous for vital cell population and cell seeding efficiency. A further increase in initial cell population showed no further benefit, regarding the vital cell population at the end of observation period. Moreover, the subsequent histological analysis of seeded scaffolds could demonstrate the population of cells on the surface of scaffolds in vital cell layers and an even distribution along the surface of the scaffold.

Interestingly, scaffolds with optimized cell seeding numbers showed vital cells between the trabeculae of the scaffolds.

There are some studies evaluating positive effects of bone allografts combined with stem cells [24, 29] but none of these

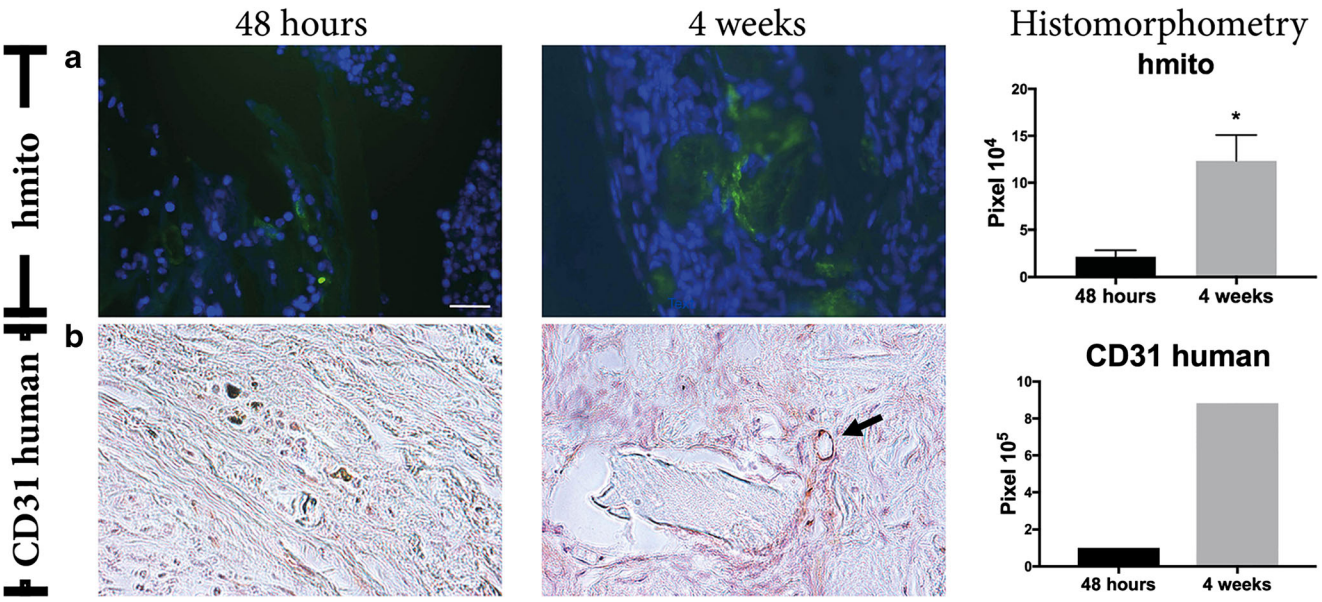

Fig. 7 Immunohistochemical stainings against human antigen of seeded and unseeded scaffolds. Antibody against human mitochondrias (hmito) showed increase of human cells within the scaffold, indicating proliferation of seeded human stem cells (**a**). Moreover, stainings against CD31-human point to endothelial differentiation of stem cells (**b**). Black arrow indicates CD31-positive cells. Results are shown as mean ± SD. *P* value: * < 0.05. Images were taken at × 20 magnification; scale bar represents 50 μm

studies systematically evaluated the ideal number of ASCs for cell seeding of bone allografts.

Further studies looking for an adequate bone replacement therapy, already provided growing evidence, that scaffolds need to be combined with cells [36, 37].

Results of in vivo experiments showed elevated bone formation within the hASC-seeded scaffolds compared with control. Moreover, immunohistochemical stainings indicated increased osteogenesis induced by hASCs. Interestingly, the amount of human cells increased over time, indicating a high conductivity of bone allograft scaffolds.

Accordingly, Kloeters et al. [29] examined ASC-seeded bone allografts in rabbits and were able to show the pro-osteogenic effects of this co-culture. In addition, Schubert et al. [38] examined bone allografts colonized with ASCs and BMSCs in a murine ectopic implantation model. Interestingly, osteogenic-differentiated ASCs in combination with bone allografts seemed to be very promising for bone graft substitutes. In contrast to our study, ASCs in this study were differentiated osteogenically in vitro before transplantation. Furthermore, different studies applying ASCs, not only as co-culture, combined with bone allografts, but synthetic scaffold materials for bone tissue engineering, indicated enhancement of osteogenesis and angiogenesis [28, 29, 39].

Potential disadvantages regarding the use of human bone allografts are mainly related to concerns about potential transmission of infectious diseases. In this context, HIV and hepatitis C constitute infections, which were particularly described in the past [40]. As a crucial advantage of freeze-dried allografts compared with freshly frozen ones, they have been proven to show less immunogenic potential and to date no HIV infection [41].

Interestingly, we could detect human and mouse endothelial cells within the seeded scaffold, so autocrine and paracrine effects of transplanted stem cells, leading to an enhanced angiogenesis, could be discussed. Accordingly, Behr et al. observed paracrine and cell-autonomous effects of VEGF-A-treated hASCs leading to endothelial differentiation [42]. In order to further validate these results, additional experiments are needed as our results only show preliminary data, which indicate endothelial differentiation of implanted hASCs.

One of the most promising synthetic scaffold materials β-tricalcium-phosphate showed good properties in osteoconductivity and mechanical strength [34, 37]. However, focusing on osseointegration, the rapid absorption of β-TCP also leads to a loss of the scaffold structure, as a long-term follow-up study could show [43].

In light of the huge variety of different scaffold materials, bone allografts co-cultured with ASCs pose a promising technique in the field of bone tissue engineering and will certainly be of great interest in the near future. Moreover, stem cell-seeded scaffolds could be used for bony defects in orthopedic surgery in a potential one-step procedure containing stem cell harvesting, scaffold seeding, and implantation in one surgery.

Recently, a further step was made, establishing stem cell-based approaches into clinical therapy by Saxer et al. examining ceramic scaffolds with SVF cells taken from lipoaspirates in hip fractures of elderly patients [44].

Besides that, clinical safety of application of ASCs in bone replacement therapy has already been demonstrated [45]. In conclusion, this study provides important findings about the optimized cell/volume ratio which further support future studies establishing of ASC-seeded bone allografts for clinical bone replacement therapy.

Seeded scaffolds showed extensively enhanced new bone formation in comparison with unseeded scaffolds after an observation period of 4 weeks. Osteocalcin positive stainings are indicated by black arrows (**a**). Histomorphometry revealed highly statistically significant differences (**b**). X-ray scans of seeded and unseeded scaffolds (**c**). Results are shown as mean ± SD. ***P value < 0.001. Images were taken at × 10 magnification; scale bar represents 100 μm

Compliance with ethical standards

All experiments were performed in adherence to the National Institute of Health guidelines for the use of experimental animals and after approval by the German legislation. The protocol was approved by the LANUV (NRW, Germany; Permit-Number: AZ 84-02.04.2013.A362).

Abbreviations *hASC*, human adipose stem cell; *DMEM*, Dulbecco's Modified Eagle Medium; *FCS*, fetal calf serum; *DIZG*, Deutsches Institut für Zell- und Gewebeersatz; *CCK-8*, cell counting kit 8; *PBS*, phosphate buffered saline; *EDTA*, Ethylenediamine-tetraacetate; *PCNA*, Proliferating-Cell-Nuclear-Antigen; *RUNX2*, Runt-related transcription factor; *DAPI*, 4,6-diamidino-2-phenylindole; *Tunel*, TdT-mediated dUTP-biotin nick end labeling; *hmito*, human mitochondrias; *HIV*, human immunodeficiency virus; *VEGF*, vascular endothelial growth factor; TCP, tricalcium-phosphate; *SVF*, stromal vascular fraction

References

1. Marelli B, Ghezzi CE, Mohn D, Stark WJ, Barralet JE, Boccaccini AR, Nazhat SN (2011) Accelerated mineralization of dense collagen-nano bioactive glass hybrid gels increases scaffold stiffness and regulates osteoblastic function. Biomaterials 32:8915–8926
2. Zhao L, Weir MD, Xu HH (2010) Human umbilical cord stem cell encapsulation in calcium phosphate scaffolds for bone engineering. Biomaterials 31:3848–3857
3. Cai L, Wang Q, Gu C, Wu J, Wang J, Kang N, Hu J, Xie F, Yan L, Liu X, Cao Y, Xiao R (2011) Vascular and micro-environmental influences on MSC-coral hydroxyapatite construct-based bone tissue engineering. Biomaterials 32:8497–8505
4. Webster TJ, Ergun C, Doremus RH, Siegel RW, Bizios R (2000) Enhanced functions of osteoblasts on nanophase ceramics. Biomaterials 21:1803–1810
5. Huang Y, Jin X, Zhang X, Sun H, Tu J, Tang T, Chang J, Dai K (2009) In vitro and in vivo evaluation of akermanite bioceramics for bone regeneration. Biomaterials 30:5041–5048

6. Rezwan K, Chen QZ, Blaker JJ, Boccaccini AR (2006) Biodegradable and bioactive porous polymer/inorganic composite scaffolds for bone tissue engineering. Biomaterials 27:3413–3431
7. Fu S, Ni P, Wang B, Chu B, Zheng L, Luo F, Luo J, Qian Z (2012) Injectable and thermo-sensitive PEG-PCL-PEG copolymer/collagen/n-HA hydrogel composite for guided bone regeneration. Biomaterials 33:4801–4809
8. Drury JL, Mooney DJ (2003) Hydrogels for tissue engineering: scaffold design variables and applications. Biomaterials 24:4337–4351
9. Mata A, Geng Y, Henrikson KJ, Aparicio C, Stock SR, Satcher RL, Stupp SI (2010) Bone regeneration mediated by biomimetic mineralization of a nanofiber matrix. Biomaterials 31:6004–6012
10. Bhakta G, Rai B, Lim ZX, Hui JH, Stein GS, van Wijnen AJ, Nurcombe V, Prestwich GD, Cool SM (2012) Hyaluronic acid-based hydrogels functionalized with heparin that support controlled release of bioactive BMP-2. Biomaterials 33:6113–6122
11. Patterson J, Siew R, Herring SW, Lin AS, Guldberg R, Stayton PS (2010) Hyaluronic acid hydrogels with controlled degradation properties for oriented bone regeneration. Biomaterials 31:6772–6781
12. Jha AK, Xu X, Duncan RL, Jia X (2011) Controlling the adhesion and differentiation of mesenchymal stem cells using hyaluronic acid-based, doubly crosslinked networks. Biomaterials 32:2466–2478
13. Bae MS, Yang DH, Lee JB, Heo DN, Kwon YD, Youn IC, Choi K, Hong JH, Kim GT, Choi YS, Hwang EH, Kwon IK (2011) Photo-cured hyaluronic acid-based hydrogels containing simvastatin as a bone tissue regeneration scaffold. Biomaterials 32:8161–8171
14. Kanczler JM, Ginty PJ, White L, Clarke NM, Howdle SM, Shakesheff KM, Oreffo RO (2010) The effect of the delivery of vascular endothelial growth factor and bone morphogenic protein-2 to osteoprogenitor cell populations on bone formation. Biomaterials 31:1242–1250
15. Park SH, Gil ES, Kim HJ, Lee K, Kaplan DL (2010) Relationships between degradability of silk scaffolds and osteogenesis. Biomaterials 31:6162–6172
16. Bhumiratana S, Grayson WL, Castaneda A, Rockwood DN, Gil ES, Kaplan DL, Vunjak-Novakovic G (2011) Nucleation and growth of mineralized bone matrix on silk-hydroxyapatite composite scaffolds. Biomaterials 32:2812–2820
17. Zhang Y, Wu C, Friis T, Xiao Y (2010) The osteogenic properties of CaP/silk composite scaffolds. Biomaterials 31:2848–2856
18. Bi L, Cheng W, Fan H, Pei G (2010) Reconstruction of goat tibial defects using an injectable tricalcium phosphate/chitosan in combination with autologous platelet-rich plasma. Biomaterials 31:3201–3211
19. Wang L, Stegemann JP (2010) Thermogelling chitosan and collagen composite hydrogels initiated with beta-glycerophosphate for bone tissue engineering. Biomaterials 31:3976–3985
20. Yu HS, Won JE, Jin GZ, Kim HW (2012) Construction of mesenchymal stem cell-containing collagen gel with a macrochanneled polycaprolactone scaffold and the flow perfusion culturing for bone tissue engineering. BioRes open access 1:124–136
21. Aravamudhan A, Ramos DM, Nip J, Harmon MD, James R, Deng M, Laurencin CT, Yu X, Kumbar SG (2013) Cellulose and collagen derived micro-nano structured scaffolds for bone tissue engineering. J Biomed Nanotechnol 9:719–731
22. Bueno EM, Glowacki J (2009) Cell-free and cell-based approaches for bone regeneration. Nat Rev Rheumatol 5:685–697
23. Zimmermann G, Wagner C, Schmeckenbecher K, Wentzensen A, Moghaddam A (2009) Treatment of tibial shaft non-unions: bone morphogenetic proteins versus autologous bone graft. Injury 40(Suppl 3):S50–S53
24. Bertolai R, Catelani C, Aversa A, Rossi A, Giannini D, Bani D (2015) Bone graft and mesenchimal stem cells- clinical observations and histological analysis. Clin Cases Miner Bone Metab 12:183–187
25. Stevenson S, Li XQ, Martin B (1991) The fate of cancellous and cortical bone after transplantation of fresh and frozen tissue-antigen-matched and mismatched osteochondral allografts in dogs. J Bone Joint Surg Am 73:1143–1156
26. Khan SN, Cammisa FP Jr, Sandhu HS, Diwan AD, Girardi FP, Lane JM (2005) The biology of bone grafting. J Am Acad Orthop Surg 13:77–86
27. Sundelacruz S, Kaplan DL (2009) Stem cell- and scaffold-based tissue engineering approaches to osteochondral regenerative medicine. Semin Cell Dev Biol 20:646–655
28. Romagnoli C, Brandi ML (2014) Adipose mesenchymal stem cells in the field of bone tissue engineering. World journal of stem cells 6:144–152
29. Kloeters O, Berger I, Ryssel H, Megerle K, Leimer U, Germann G (2011) Revitalization of cortical bone allograft by application of vascularized scaffolds seeded with osteogenic induced adipose tissue derived stem cells in a rabbit model. Arch Orthop Trauma Surg 131:1459–1466
30. Zwingenberger S, Niederlohmann E, Vater C, Rammelt S, Matthys R, Bernhardt R, Valladares RD, Goodman SB, Stiehler M (2013) Establishment of a femoral critical-size bone defect model in immunodeficient mice. J Surg Res 181:e7–e14
31. Behr B, Leucht P, Longaker MT, Quarto N (2010) Fgf-9 is required for angiogenesis and osteogenesis in long bone repair. PNAS 107:11853–11858
32. Wallner C, Schira J, Wagner JM, Schulte M, Fischer S, Hirsch T, Richter W, Abraham S, Kneser U, Lehnhardt M, Behr B (2015) Application of VEGFA and FGF-9 enhances angiogenesis, osteogenesis and bone remodeling in type 2 diabetic long bone regeneration. PLoS One 10:e0118823
33. Wagner JM, Reinkemeier F, Wallner C, Dadras M, Huber J, Schmidt SV, Drysch M, Dittfeld S, Jaurich H, Becerikli M, Becker K, Rauch N, Duhan V, Lehnhardt M, Behr B (2019) Adipose derived stromal cells (ASCs) are capable to restore bone regeneration after posttraumatic osteomyelitis and modulate B-cell response. Stem Cells Transl Med. https://doi.org/10.1002/sctm.18-0266
34. Seebach C, Schultheiss J, Wilhelm K, Frank J, Henrich D (2010) Comparison of six bone-graft substitutes regarding to cell seeding efficiency, metabolism and growth behaviour of human mesenchymal stem cells (MSC) in vitro. Injury 41:731–738
35. Zuk PA, Zhu M, Mizuno H, Huang J, Futrell JW, Katz AJ, Benhaim P, Lorenz HP, Hedrick MH (2001) Multilineage cells from human adipose tissue: implications for cell-based therapies. Tissue Eng 7:211–228
36. Polo-Corrales L, Latorre-Esteves M, Ramirez-Vick JE (2014) Scaffold design for bone regeneration. J Nanosci Nanotechnol 14:15–56
37. Seebach C, Henrich D, Wilhelm K, Barker JH, Marzi I (2012) Endothelial progenitor cells improve directly and indirectly early vascularization of mesenchymal stem cell-driven bone regeneration in a critical bone defect in rats. Cell Transplant 21:1667–1677
38. Schubert T, Xhema D, Veriter S, Schubert M, Behets C, Delloye C, Gianello P, Dufrane D (2011) The enhanced performance of bone allografts using osteogenic-differentiated adipose-derived mesenchymal stem cells. Biomaterials 32:8880–8891
39. Morcos MW, Al-Jallad H, Hamdy R (2015) Comprehensive review of adipose stem cells and their implication in distraction osteogenesis and bone regeneration. BioMed research international 2015:842975
40. Conrad EU, Gretch DR, Obermeyer KR, Moogk MS, Sayers M, Wilson JJ, Strong DM (1995) Transmission of the hepatitis-C virus by tissue transplantation. J Bone Joint Surg Am 77:214–224

41. Ehrler DM, Vaccaro AR (2000) The use of allograft bone in lumbar spine surgery. Clin Orthop Relat Res 371:38–45
42. Behr B, Tang C, Germann G, Longaker MT, Quarto N (2011) Locally applied vascular endothelial growth factor A increases the osteogenic healing capacity of human adipose-derived stem cells by promoting osteogenic and endothelial differentiation. Stem Cells 29:286–296
43. Thesleff T, Lehtimaki K, Niskakangas T, Huovinen S, Mannerstrom B, Miettinen S, Seppanen-Kaijansinkko R, Ohman J (2017) Cranioplasty with adipose-derived stem cells, beta-tricalcium phosphate granules and supporting mesh: six-year clinical follow-up results. Stem Cells Transl Med 6:1576–1582
44. Saxer F, Scherberich A, Todorov A, Studer P, Miot S, Schreiner S, Guven S, Tchang LA, Haug M, Heberer M et al (2016) Implantation of stromal vascular fraction progenitors at bone fracture sites: from a rat model to a first-in-man study. Stem Cells 34: 2956–2966
45. Veriter S, Andre W, Aouassar N, Poirel HA, Lafosse A, Docquier PL, Dufrane D (2015) Human adipose-derived mesenchymal stem cells in cell therapy: safety and feasibility in different "hospital exemption" clinical applications. PLoS One 10:e0139566